Determining CO2 storage efficiency within a saline aquifer using reduced complexity models

de Jonge-Anderson, Iain; Ramachandran, Hariharan; Nicholson, Uisdean; Geiger, Sebastian; Widyanita, Ana; Doster, Florian

DOI
10.46690/ager.2024.07.04

Publication date
2024

Document Version
Final published version

Published in
Advances in Geo-Energy Research

Citation (APA)
de Jonge-Anderson, I., Ramachandran, H., Nicholson, U., Geiger, S., Widyanita, A., & Doster, F. (2024). Determining CO2 storage efficiency within a saline aquifer using reduced complexity models. *Advances in Geo-Energy Research*, *13*(1), 22-31. https://doi.org/10.46690/ager.2024.07.04

Advances in Geo-Energy Research

Vol. 13, No. 1, p. 22-31, 2024

Original article

Determining CO_2 storage efficiency within a saline aquifer using reduced complexity models

Iain de Jonge-Anderson[1]*, Hariharan Ramachandran[1], Uisdean Nicholson[1], Sebastian Geiger[2], Ana Widyanita[3], Florian Doster[1]

[1]*Institute of GeoEnergy Engineering, Heriot-Watt University, Edinburgh EH14 4AS, UK*

[2]*Faculty of Civil Engineering and Geosciences, Technische Universiteit Delft, South Holland 2628 CN Delft, Netherlands*

[3]*PETRONAS Research Sdn. Bhd., Selangor43000, Malaysia*

Keywords:
Carbon capture and storage
storage capacity
vertical equilibrium models
trap analysis
Malay Basin

Cited as:
de Jonge-Anderson, I., Ramachandran, H., Nicholson, U., Geiger, S., Widyanita, A., Doster, F. Determining CO_2 storage efficiency within a saline aquifer using reduced complexity models. Advances in Geo-Energy Research, 2024, 13(1): 22-31. https://doi.org/10.46690/ager.2024.07.04

Abstract:
Carbon capture and storage is vital for reducing greenhouse gas emissions and mitigating climate change. Most projects involve the permanent geological storage of CO_2 within deep sedimentary rock formations, but accurately constraining storage capacity usually involves detailed and computationally demanding reservoir modeling and simulation. Efficiency factors can also be used but these often lead to capacity overestimations. To address this, a workflow is proposed harnessing various existing, reduced complexity models that account for the surface topography and dynamic fluid behavior in a computationally efficient manner. This workflow was tested in an area of the Malay Basin mapped from three-dimensional seismic data but with illustrative reservoir parameters. A static analysis was first undertaken using algorithms within MRST-co2lab. Structural traps, spill paths and spill regions were identified using the reservoir topography. This provided initial indications into optimal well placement and led to refinement of the total capacity of the area into the capacity available within structural traps. This was followed with a dynamic analysis, also within MRST-co2lab, using computationally efficient Vertical Equilibrium models. Hundreds of simulations were undertaken and the optimal well placement was determined based on the maximum storage efficiency achieved. The results indicated that the amount that can be contained within this area is 15 times less than equivalent predictions using static storage efficiency factors. The advantage of such a light approach is that sensitivity and uncertainty analysis can be carried out at speed, before targeting certain parameters/areas for more detailed study.

1. Introduction

The permanent storage of CO_2 within deep geological formations is critical for achieving significant reductions in greenhouse gas emissions and mitigating climate change (IPCC, 2023). However, evaluating the capacity of a geological storage site is a complex task, involving various approaches and definitions. During the initial stages of a project, capacity estimates often overlook the dynamic behavior of a reservoir, favoring a volumetric approach that considers only the static pore volume available for storage (Bachu et al., 2007). This approach may lead to overestimations of capacity if factors such as pressure evolution and compressibility are neglected (Thibeau and Mucha, 2011).

Efficiency factors play a crucial role in constraining storage capacity during screening processes. They are used to parameterize dynamic reservoir effects and represent the proportion of the reservoir's pore space that can be accessed by CO_2, considering geology (permeability, connectivity, etc.) and other subsurface and operational criteria including pressure, injection strategy, and regulatory constraints (Nordbotten and Celia, 2011; Bachu, 2015; Mathias et al., 2015). They are widely utilized in national and international CO_2 storage screening programs including those in the UK, USA, and Eur-

Yandy Scientific Press

*Corresponding author.
E-mail address: i.anderson@hw.ac.uk (I. de Jonge-Anderson); h.ramachandran@hw.ac.uk (H. Ramachandran); u.nicholson@hw.ac.uk (U. Nicholson); S.Geiger@tudelft.nl (S. Geiger); ana.widyanita@petronas.com (A. Widyanita).

Received March 15, 2024; revised April 20, 2024; accepted May 16, 2024; available online May 22, 2024.

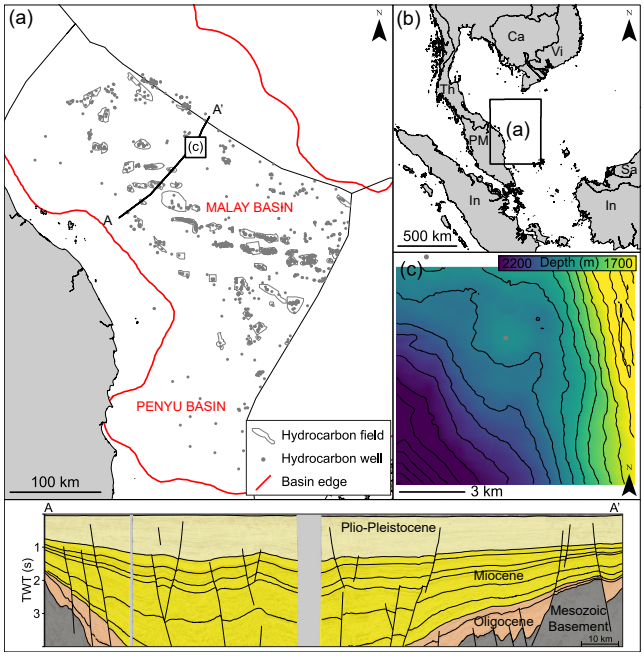

Fig. 1. (a) Map of offshore Peninsular Malaysia showing the outlines of major sedimentary basins, hydrocarbon fields, wells, and the locations of (c) and cross-section A-A', (b) inset map showing (a)'s position in relation to the wider Southeast Asia region and (c) top reservoir surface map in the J Area. A-A': Seismic cross-section showing the main stratigraphic units (after de Jonge-Anderson et al. (2024)). Ca: Cambodia, In: Indonesia, PM: Peninsular Malaysia, Th: Thailand, TWT: two-way-time, Vi: Vietnam.

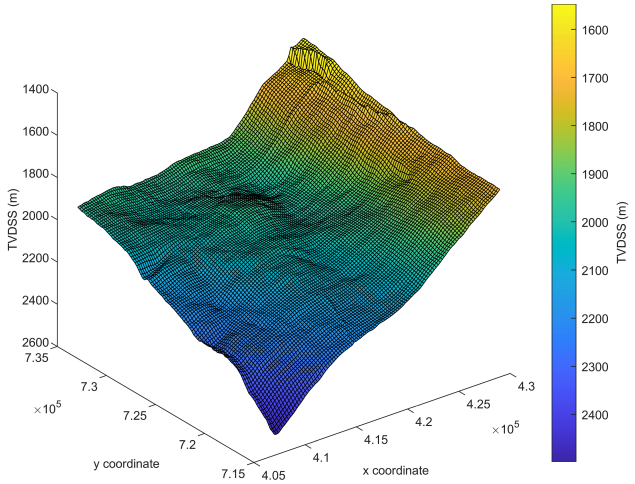

Fig. 2. The top surface grid used for trap analysis and simulations.

ope (Vangkilde-Pedersen et al., 2009; Goodman et al., 2011; Bentham et al., 2014). However, the selection of appropriate efficiency factors is often done based on analogue reservoirs, introducing a degree of ambiguity in their application.

Full physics reservoir simulators, traditionally used to quantify fluid flow and pressure response within a reservoir, require extensive knowledge of the subsurface, which is often challenging and costly to obtain, particularly at the early stages of a project. There has been much research effort to expedite this process such as using analytical equations for fluid flow (Nordbotten et al., 2005; Okwen et al., 2010) or sketch-based reservoir models (Jackson et al., 2022). As a compromise between full physics simulations and analytical expressions, Vertical Equilibrium (VE) models have emerged as effective tools for representing CO_2 plume behavior (Gasda et al., 2009; Nilsen et al., 2011, 2016; Nordbotten and Celia, 2011; Lie et al., 2016). By simplifying the governing equations into a lower-dimensional system, VE models significantly reduce computational complexity while still providing valuable insights into storage behavior.

In this study, we report on an improved workflow for estimating CO_2 storage efficiency by incorporating published static and dynamic reduced complexity models. This approach yields more realistic capacity estimates when compared to traditional static equation-based estimates. To illustrate this approach, we apply our workflow to a small area of the Malay Basin, offshore Peninsular Malaysia ("J Area") (Fig. 1). The Malay Basin is a mature hydrocarbon province that has substantial CO_2 storage potential. The storage capacity within saline aquifers alone is estimated at 84-114 Gt (Hasbollah et al., 2020), while depleted fields could offer a further 3.8 Gt of storage (APEC, 2005). However, despite the wealth of data from decades of exploration and production, there is still substantial uncertainty about how a CO_2 plume and its associated pressure buildup will interact with geological structures (anticlines and faults), heterogeneous reservoir distributions, and variable seal efficacies. This will ultimately lead to errors in calculating storage capacity, particularly in saline aquifers with less subsurface data available.

We aim to estimate the effective storage capacity of the J Area with limited subsurface data, but without relying on static and generalized efficiency factors. We focus on assessing the impacts of reservoir topography and injection well location on plume behavior and storage containment, utilizing a physics-informed yet computationally efficient workflow within the MRST-co2lab framework (Andersen et al., 2016; Lie, 2019). By adopting this approach, we aim to provide insights that could inform CO_2 storage assessments in other basins with limited data availability.

2. Data and methodology

2.1 Structural grid

We first interpreted a time-domain three-dimensional (3D) seismic dataset and created a surface corresponding to the top of the candidate reservoir (Fig. 2). A high-amplitude seismic reflector was auto-tracked and gridded at a 200 m by 200 m (X and Y) resolution. The surface was then depth-converted using a single-layer velocity model constrained by checkshot data (de Jonge-Anderson et al., 2024). For our analysis, a simple 3D grid was constructed by duplicating this surface, shifting the duplicated surface 1,000 m deeper, and then creating five equally spaced layers between, resulting in a grid with dimensions of 200 m × 200 m × 200 m (Table 1).

Table 1. Model information.

Type	Property	Value
Grid	Number of cells (NX × NY × NZ)	$100 \times 110 \times 5$
	Cell dimensions (DX × DY) (m)	200×200
	Area (km^2)	440 (22×20)
	Average top reservoir depth (m)	1,984.00
	Seafloor temperature (°C)[a]	24.00
	Temperature gradient (°C/km)[a]	50.00
	Water depth (m)	70.00
Rock	Porosity	0.05-0.25 (arithmetic mean = 0.15)
	Permeability (mD)	1.20-241.00 (arithmetic mean = 39.40)
	Rock compressibility (Pa^{-1})	4.35×10^{-10}
Fluid (at 2,000 m depth)	Brine viscosity (Pa.s)[b]	3.13×10^{-4}
	Brine density (kg/m^3)[b]	1,001.00
	Brine salinity (ppm)	70,000
	Brine compressibility (Pa^{-1})	0
	CO_2 viscosity (Pa.s)[c]	3.21×10^{-5}
	CO_2 density (kg/m^3)[d]	389.70
	CO_2 compressibility (Pa^{-1})	5.78×10^{-8}
Rock-fluid	Residual gas (CO_2) saturation	0.20
	Irreducible water saturation	0.27
	Relative permeability model	$(s_g - s_{gr})^2 / (1 - s_{gr})^2$

Notes: [a]Data from Madon and Jong (2021); [b]Data from Batzle and Wang (1992); [c]Data from Fenghour et al. (1998); [d]Data from Span and Wagner (2003). s_g: Gas saturation, s_{gr}: Residual gas saturation.

2.2 Structural trapping analysis

The identification of traps was conducted using MRST-co2lab, employing an edge-based approach that treats the top surface of the grid as a network of nodes (grid corners) and edges (connections between nodes) with flow occurring along the edges (Nilsen et al., 2015, see trapAnalysis.m in the MRST 2023b co2lab module). This method returns a trapping framework that identifies cells belonging to either a structural trap, spill path or spill region (Nilsen et al., 2015; Lie et al., 2016). Structural traps correspond to local maxima in the top surface (a structural high). Traps are connected by spill paths that connect each node to its upslope neighbor, ultimately leading to a local maximum or the edge of the model. Each structural trap is surrounded by a spill region; essentially a catchment area that feeds the given trap.

2.3 Vertical equilibrium model

VE modeling is a well-established approach to simulating the injection and storage of CO_2 (Nordbotten and Celia, 2006; Gasda et al., 2009; Nordbotten et al., 2009; Juanes et al., 2010; Nilsen et al., 2011; Nordbotten and Celia, 2011; Lie et al., 2016). The governing equations are outlined in many of these studies and are not repeated herein; however, we shall briefly describe the theorical background for completeness. The theory is anchored in the assumption of vertical equilibrium: In a two-phase system, if one phase (CO_2) is significantly lighter than the other (brine), a strong buoyant drive on the light phase leads to vertical segregation on a timescale much faster than that required for lateral migration. Under these conditions, CO_2 forms a thin layer immediately beneath the caprock, and the vertical distribution of the plume can be approximated by buoyancy and capillary forces. Hence, plume height can be expressed as an analytical function and plume migration simulated as a 2D rather than a 3D problem. The strength of the VE modeling approach lies in its computational efficiency, with simulations typically running much faster than traditional 3D reservoir simulations. It has also been extensively validated, for example against 3D reservoir simulations (Nilsen et al., 2011) and benchmark models (Nilsen et al., 2017). We implemented a VE model within the black-oil type framework typically used within the petroleum industry

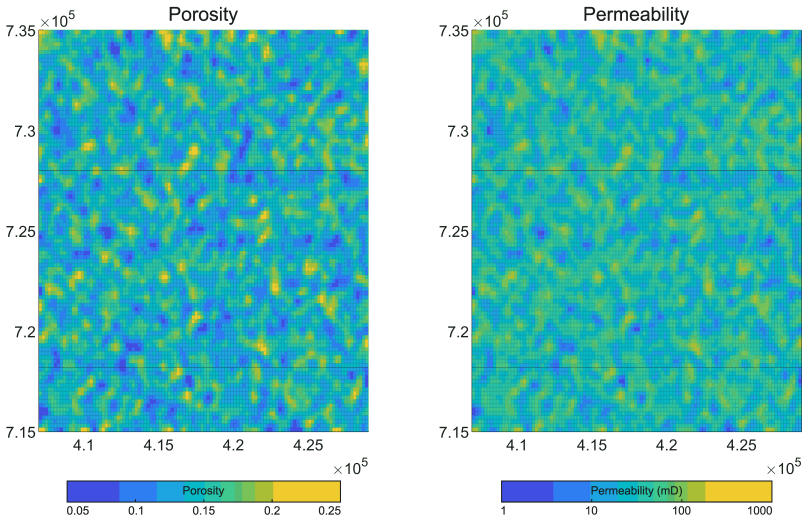

Fig. 3. Porosity (left) and permeability (right) distributions for the top reservoir surface. The porosity distribution was created by a Gaussian field with limits of between 0.05 and 0.25 and a standard deviation of 0.02. The permeability distribution was estimated from porosity using the Carman-Kozeny empirical relationship (Carman, 1937).

(Nilsen et al., 2016, see CO2VEBlackOilTypeModel.m in the MRST 2023b co2lab module).

2.3.1 Petrophysical and fluid model

The gross reservoir interval comprises a heterogeneous and thick sequence of lower to middle Miocene sandstones, mudstones, and coals. During the early to middle Miocene, The J Area was situated in a coastal plain-to-shoreface setting, close to sea level, with sandstone beds representing offshore sand bars, fluvial channels, or estuarine channels. Although no core or cuttings data were available for this area, published regional data suggest that sandstone reservoirs in the basin typically have porosities ranging between 0.1 and 0.2 (Kuttan et al., 1980).

For the petrophysical model, porosity values were assigned to each grid cell using a Gaussian field with bounds of 0.05 and 0.25 with a standard deviation of 0.02 (Fig. 3). Permeability values were estimated from porosity using the Carman-Kozeny empirical relationship (Carman, 1937). Since there was no specific information available to determine irreducible water saturation, it was fixed at 0.27, falling within the typical range of 0.2-0.4 for water-wet sandstones (Baker et al., 2015).

For the fluid model, we assumed a hydrostatic pressure gradient of 10 MPa/km and a temperature gradient of 50 °C/km (Madon and Jong, 2021). Reference density, viscosity and compressibility values for CO_2 and brine were calculated using appropriate equations of state (Table 1) and fine-scale capillary behavior was included using a P-scaled table, which approximates a capillary fringe based on upscaled capillary pressure (Nilsen et al., 2016).

2.3.2 Simulation schedule

A schedule consisting of 128 timesteps was created starting with 30, 1-year timesteps corresponding to the injection period, followed by 95, 10-year timesteps corresponding to the post-injection period (1,000 years in total). Hydrostatic conditions were assigned to the boundary cells of the grid, allowing brine and CO_2 to flow out of the grid where necessary. For the purposes of this study, the edges of the grid were considered as pseudo-storage license boundaries, making lateral migration of CO_2 outside of the grid undesirable. During the injection period, a single well was used to inject 1 Mt of CO_2 per year into the grid.

2.3.3 Maximizing storage efficiency

The computational efficiency of VE models enabled us to rapidly conduct multiple simulations and test various uncertainties. For this study, we conducted a systematic analysis to determine the optimal location for an injection well in the area assuming the best location is where the highest storage efficiency is achieved. We first calculated the CO_2 volume v_{CO_2} remaining within the grid at the end of the migration period and divided this by the total pore volume of the grid v_P. The storage efficiency ε was then defined as:

$$\varepsilon = \frac{v_{CO_2}}{v_P} \times 100 \quad (1)$$

A simulation was performed with an injection well at every 25th grid cell, resulting in 440 simulations across the 11,000-cell top surface grid. Each iteration ran in around 45 seconds on an Intel Xeon Gold 6240R 2.4 GHz CPU. Our objective was to determine which of these 440 injection locations minimized leakage away from the model boundary and, in doing so, maximized the amount of CO_2 being stored within the area, and the storage efficiency ε.

3. Results

3.1 Spill point analysis

The total rock volume in our model was determined to be 440,000 Mm^3. However, only a subset of this volume consists

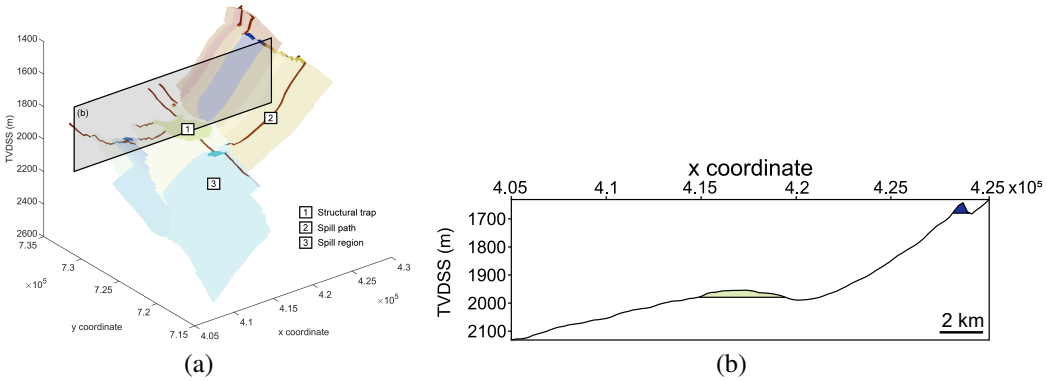

(a) (b)

Fig. 4. (a) Map of structural traps, spill paths, and spill regions identified using the "Trap Analysis" function in MRST-co2lab and (b) cross-section through the top surface grid highlighting two structural closures separated by a strongly tilted region. The location of the line is shown in (a).

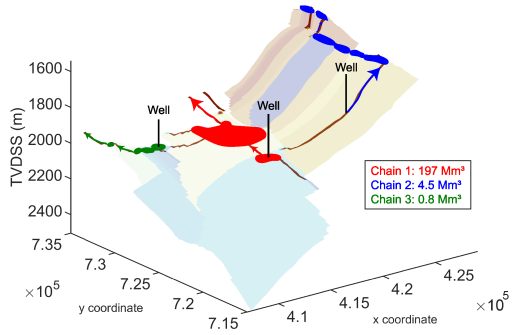

Fig. 5. Map of trapping framework (as per Fig. 4) with three contrasting trapping chains and their associated trapping volumes.

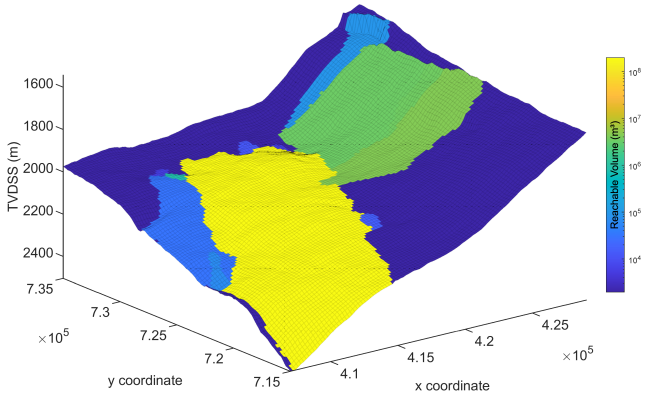

Fig. 6. Map of the top structure grid colored by reachable volume, i.e., the volume of the grid cells within structural closures that are up-dip from that cell.

of structures suitable for the structural trapping of CO_2. These structural traps play a vital role in short-term trapping CO_2 trapping before other trapping mechanisms, such as residual, solubility, and mineral trapping, occur. A static trapping framework for the J Area was developed (Fig. 4), and from this, we calculated the rock volume within structural traps (along the top structure grid, only) as 202 Mm^3. The area dips to the southwest with an anticline in the center (Figs. 2 and 4). The anticline, at 195 Mm^3, accounts for 97% of the entire structural trapping volume of the area. The remaining 3% is spread mainly across four smaller traps of between 0.8 and 3.3 Mm^3, with the rest held within traps down to almost negligible volumes (< 0.01 Mm^3).

3.2 Trapping chains

An initial understanding of the ideal well placement was first gained from analyzing the trapping chains within the system. Trapping chains are essentially a series of traps that could be accessed within a "fill and spill" injection scenario. In this scenario, we assume infinite CO_2 injection allowing any trap along a migration pathway to be fully filled before CO_2 spills and moves into the next trap (or outside of the grid). In doing this, no injection simulations are performed but a concept emerges as to how to access the maximum trapping structure within a static analysis framework (Nilsen et al., 2015).

Fig. 5 illustrates three well placements with contrasting trapping chains. In the first example (highlighted in red at the center of the grid), a well is placed within a small trap downdip of the anticline. If this trap were filled to spill, CO_2 would migrate into and fill the anticline before leaving the model to the north. This results in most of the trapping volume of the grid being accessed (197 Mm^3). By contrast, placing injection wells in either the downdip west (green) or updip east (blue) areas, results in CO_2 migration into only small structures (4.5 and 0.8 Mm^3, respectively).

This concept is conceptualized as a "reachable volume": The total trapping volume that can be accessed from a given grid cell. Fig. 6 illustrates the grid with coloring corresponding to the reachable volume of that cell. Here, the anticline and the region downdip and to the southwest of it is the optimal well location considering purely the volume of traps accessed.

3.3 Vertical equilibrium modeling

The analysis undertaken so far provides valuable insights into the optimal placement of an injection well in the area, primarily based on a static analysis of the geometry of the top surface. However, the impact of the reservoir's petrophysical

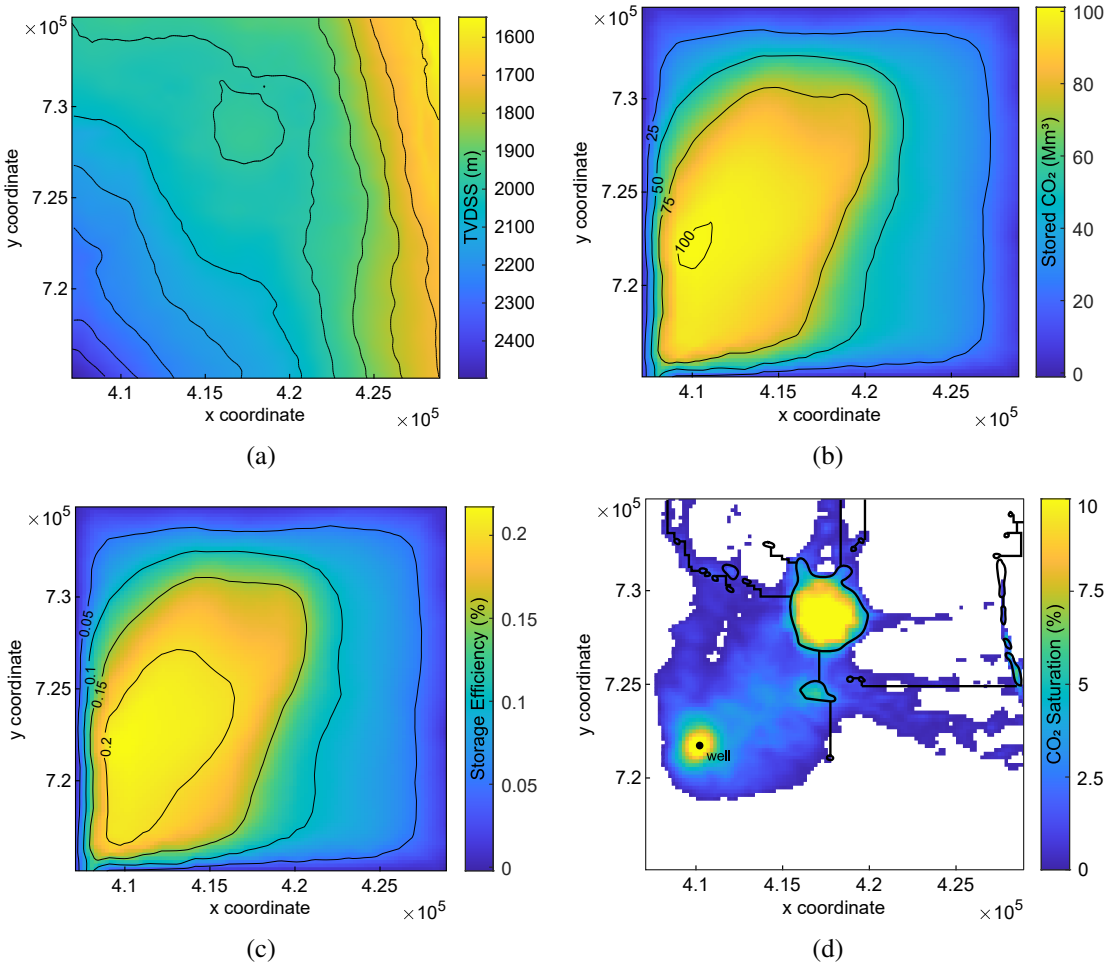

Fig. 7. Output maps from the VE modeling showing (a) the top structure of the reservoir, (b) stored CO_2 volume, (c) storage efficiency and (d) the final saturation distribution of CO_2 for the optimal well location.

Table 2. Summary of CO_2 capacities determined at each stage of our analysis.

Calculation type	Capacity description	Capacity (Mm^3)
Entire grid	Total rock volume	440,000
	Total pore volume	63,794
Structural trapping (along top surface*)	Total pore volume within structural traps	29
VE model	Trapped CO_2 volume (max)	101.27
	Trapped CO_2 volume (min)	0.77

Notes: *Structural trapping is only calculated for the top surface of the grid, so it is significantly smaller than other volume metrics.

properties on the flow behavior and migration of CO_2 has not yet been considered. To address this, we utilized a VE model to simulate injection, as outlined in Section 2.3. This necessitated static petrophysical models of porosity and permeability (Fig. 3). Accounting for these models, the area's total pore volume is 63,794 Mm^3, capable of storing approximately 25 Gt of CO_2, assuming the CO_2 density listed in Table 1.

The total trapped CO_2 volume and storage efficiency were mapped from the results of all the simulations (Figs. 7(b) and 7(c)). The amount of CO_2 stored within the model at the end of the simulation period was variable, ranging from 0.77 to 101.27 Mm^3 (Table 2). The corresponding storage efficiencies ranged from 0.0017% to 0.22% (Fig. 7(c)).

The lowest storage efficiencies and trapped CO_2 volumes were observed near the model boundaries where most injected CO_2 exited the model domain (Fig. 7(c)). Conversely, the highest storage efficiencies and trapped CO_2 volumes were observed when the well was positioned in the lower-left side of the model (Fig. 7(c)). In these cases, a significant area of up-dip, unconfined reservoir was available for CO_2 migration, alongside an anticline that eventually formed a trap for the migrating CO_2 plume (Fig. 7(d)). Notably, injection directly into this anticline itself resulted in lower storage efficiencies and stored volumes, as the anticline was quickly filled-to-spill and the CO_2 then migrated northwards and out of the model

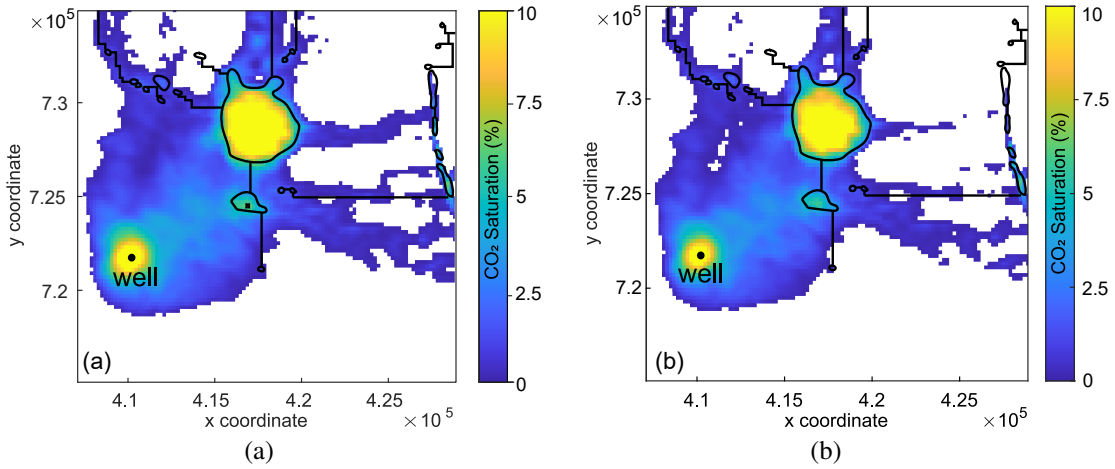

Fig. 8. Final CO_2 saturation distribution maps for (a) the simulation case with an optimized injection rate of 1.3 Mt/year and (b) the simulation case presented in this study with a fixed injection rate of 1 Mt/year.

domain.

From this analysis, we can conclude that the optimal well location was at the coordinate pair (410,100 m, 721,700 m) (Fig. 7(d)), with a storage efficiency of 0.22% and a capacity of 101.27 Mm^3 (Table 2).

4. Discussion

4.1 Comparison with static efficiency coefficients

During the site-screening stage, CO_2 storage efficiency is often estimated using coefficients or analytical solutions. Previous studies have proposed storage coefficients or classifications of storage efficiency based on numerical simulations or laboratory work, that can then be extrapolated to other aquifers based on shared characteristics (often the depositional environment, lithology, or petrophysical behavior) (Gorecki et al., 2009; Blondes et al., 2013; Brennan, 2014).

Analytical solutions, while offering rapid assessments, often make assumptions of reservoir homogeneity and/or a closed aquifer system (Zhou et al., 2008; Okwen et al., 2010; Szulczewski et al., 2012). Storage efficiency is ultimately a dynamic property that evolves with injection time (Okwen et al., 2014; Szulczewski et al., 2014). Bachu (2015) suggested that volumetric approaches to storage efficiency were adequate at the screening level, but these should be replaced at the local level by numerical simulations incorporating various operational and regulatory constraints.

In recent years, there has been significant research into developing fast tools for CO_2 storage screening utilizing VE modeling (Lie et al., 2016), sketch-based modeling (Jackson et al., 2022; Petrovskyy et al., 2023) or reduced-order models (Jin and Durlofsky, 2018). These approaches aim to overcome the limitations of traditional screening methods by providing more accurate estimates of storage capacity and efficiency, with limited data and/or resources.

In this work, we utilized VE models to enable numerical modeling at the screening stage, allowing for quick simulations of uncertain parameters and estimation of dynamic plume behavior, which is lacking in volumetric approaches to capacity/efficiency estimation. Using a conservative storage efficiency factor of 2.4% (Goodman et al., 2011) and the area properties mentioned in Table 1, the static capacity of the J Area is calculated to be 1,531.06 Mm^3. However, the results from VE modeling indicate that the amount that can be contained within the area is 15 times less, at 101.27 Mm^3 (Table 2). This result clearly shows the importance of dynamic effects and their constraint on storage capacity. Accounting for these effects is essential to avoid overestimating storage capacity, especially at the site screening phase.

4.2 Comparison with rate-controlled optimization

Our approach was compared with a previously published optimization method within MRST-co2lab which finds the optimum CO_2 injection rate using an objective function to maximize the injected CO_2 volume while minimizing migration beyond the model boundaries (Lie et al., 2016; see optimizeFormation.m function in the MRST 2023b co2lab module). In this optimization framework, any leaked CO_2 (defined as the difference between the injected CO_2 volume and the CO_2 volume retained within the grid) is subjected to "leak penalty" constant. Following the methodology outlined by Lie et al. (2016), we set this constant to 10. All rock, fluid and simulation parameters were kept the same as described in Section 2. While this optimization workflow picks an injection well location where the largest structural trapping can be achieved, we chose to override this and fix the well location at the coordinates described in Section 3.3 for a more direct comparison with our work.

After implementing this optimization procedure, the adjusted injection rate was determined to be 1.3 Mt/year. This suggests that our initial injection rates (1 Mt/year) could be slightly increased without resulting in significant amounts of CO_2 leaving the model domain. The corresponding saturation map closely resembles that resulting from the 1 Mt/year scenario (Fig. 8). However, the higher injection rate leads to

133 Mm^3 of CO_2 being stored, and a storage efficiency of 0.29%, a slight improvement on the 0.22% value obtained previously. This outcome also instils confidence in our approach, indicating that while we assessed storage efficiency based on CO_2 stored within the grid, we were not over-injecting and allowing substantial amounts of CO_2 to migrate outside of the area.

4.3 Limitations and further work

4.3.1 Inherent limitation to VE modeling

While VE modeling is a powerful and flexible tool for simulating CO_2 storage in aquifers, it is important to recognize certain inherent limitations within the model. It is assumed that CO_2 and brine segregate instantaneously in the vertical direction, but this only holds if the vertical permeability is greater than around 100 mD for injection rates and aquifer thicknesses representative for CO_2 storage sites (Court et al., 2012). Additionally, the vertical averaging of reservoir properties presents a challenge within layered reservoirs as small-scale baffles to vertical flow may not be adequately represented in subsequent modeling efforts. Recent studies have sought to adapt and develop VE models by coupling them with full dimensional simulations where necessary (Møyner and Nilsen, 2019; Becker et al., 2022). Furthermore, while some studies have incorporated mineral and dissolution trapping processes within VE models (Gasda et al., 2011; Postma et al., 2022), the approach used herein focuses solely on structural and residual trapping mechanisms. As the focus of this work are the physical trapping mechanisms, these geochemical mechanisms are neglected, although they have a substantial impact on long-term storage (De Silva et al., 2015).

4.3.2 Study-specific limitations

Our reservoir modeling approach treats the reservoir as vertically homogenous unit, assuming porosity and permeability characteristics typical of average values in the Malay Basin. However, these reservoirs are known to exhibit significant layering, comprising thin reservoir intervals separated by low-permeability mudstones. CO_2 plumes would likely be much more complex than those modeling in our study and further work could include investigating the use of hybrid-VE models (Møyner and Nilsen, 2019) to better represent this geological setting.

In our modeling case, we focused on a single well injecting CO_2 at a constant rate and open model boundaries, which allows CO_2 to freely leave the area-of-interest (pseudo-storage license). A larger model would be required to determine where this CO_2 eventually migrates to and the associated pressure response immediately outside the storage license. Including more injection wells could improve injectivity and storage efficiency, but this would be accompanied by further challenges such as that of minimizing pressure interference (Pooladi-Darvish et al., 2011).

Furthermore, we did not account for pressure evolution around the well or further afield. However, in reality, pressures must be monitored as to not exceed caprock fracture pressure. Further work could focus on understanding this pressure buildup and its influence on geomechanical properties within the reservoir and caprock. The magnitude and extent of pressure perturbation may also constrain the storage capacity of the system (Bachu, 2015; Birkholzer et al., 2015). Given the topographical variations across the top surface grid, it would be sensible to monitor reservoir pressure in the far up-dip area in the northeast to ensure these are not approaching or exceeding fracture pressures.

5. Conclusions

A workflow for assessing the storage capacity and efficiency of a saline aquifer is presented, through combining static and dynamic reduced complexity tools. These tools include static methods (automated identification of structural traps and optimization of well location to access the greatest trapping volume) and dynamic methods (VE models). In the case of the latter, the greatly reduced computational running time allows us to run optimization procedures and sensitivity analysis around uncertain parameters; an approach that cannot be undertaken with more powerful, but computationally expensive reservoir simulators. We apply these techniques to an area offshore Malaysia with illustrative reservoir parameters and focus strictly on CO_2 plume migration obtained from VE modeling. The main conclusions taken from this work are as follows:

1) Taking a volumetric approach to storage capacity results in unrealistically large values. The key finding is that the storage capacity derived from VE modeling is two orders of magnitude smaller than that derived from the total pore volume for the area.
2) The upper bound on storage efficiency is ultimately dictated by how much CO_2 is injected into the aquifer system without suffering leakage away from the model boundary (a proxy for a storage license). We analyzed well placement by performing hundreds of simulations and calculating storage efficiency. This resulted in the best location for our area being down-dip of an anticline structure into which the CO_2 would migrate during the post-injection period.
3) There is general agreement between static and dynamic approaches to well placement optimization. The area with the greatest "reachable volume" corresponds to the area highlighted by VE modeling as achieving the greatest storage efficiency, though this result could change with different porosity/permeability distributions. However, storage capacities defined by static models are still theoretical maximums and simulations should be used to assess to what extent pore space can be accessed, incorporating physics and spatial changes in geology.

Acknowledgements

The funding and data underpinning this work were provided by PETRONAS via the PETRONAS Centre of Excellence in Subsurface Engineering and Energy Transition (PACESET), based at Heriot-Watt University. Dr Raj Deo Tewari is gratefully acknowledged for providing review and constructive feedback on the manuscript. SLB is thanked for

providing an academic license for Petrel which facilitated this work. SG thanks Energi Simulation for supporting his chair.

Additional information: Author's email

F.Doster@hw.ac.uk (F. Doster).

Conflict of interest

The authors declare no competing interest.

References

Andersen, O., Lie, K. A., Nilsen, H. M. An Open-Source Toolchain for Simulation and Optimization of Aquifer-Wide CO_2 Storage. Energy Procedia, 2016, 86: 324-333.

Asia-Pacific Economic Cooperation (APEC). CO_2 storage prospectivity of selected sedimentary basins in the region of China and South East Asia, 2005.

Bachu, S. Review of CO_2 storage efficiency in deep saline aquifers. International Journal of Greenhouse Gas Control, 2015, 40: 188-202.

Bachu, S., Bonijoly, D., Bradshaw, J., et al. CO_2 storage capacity estimation: Methodology and gaps. International Journal of Greenhouse Gas Control, 2007, 1(4): 430-443.

Baker, R. O., Yarranton, H. W., Jensen, J. L. Special core analysis-Rock-fluid interactions, in Practical Reservoir Engineering and Characterization, edited by R. O. Baker, H. W. Yarranton and J. L. Jensen, Elsevier, Amsterdam, pp. 239-295, 2015.

Batzle, M., Wang, Z. Seismic properties of pore fluids. Geophysics, 1992, 57(11): 1396-1408.

Becker, B., Guo, B., Buntic, I., et al. An adaptive hybrid vertical equilibrium/full-dimensional model for compositional multiphase flow. Water Resources Research, 2022, 58(1): e2021WR030990.

Bentham, M., Mallows, T., Lowndes, J., et al. CO_2 STORage evaluation database (CO_2 Stored). The UK's online storage atlas. Energy Procedia, 2014, 63: 5103-5113.

Birkholzer, J. T., Oldenburg, C. M., Zhou, Q. CO_2 migration and pressure evolution in deep saline aquifers. International Journal of Greenhouse Gas Control, 2015, 40: 203-220.

Blondes, M. S., Brennan, S. T., Merrill, M. D., et al. National assessment of geologic carbon dioxide storage resources-methodology implementation. US Geological Survey Open-File Report, 2013.

Brennan, S. T. The US Geological Survey carbon dioxide storage efficiency value methodology: Results and observations. Energy Procedia, 2014, 63: 5123-5129.

Carman, C. P. Fluid flow through a granular bed. Transactions of the Institution of Chemical Engineers, 1937, 15: 150-156.

Court, B., Bandilla, K. W., Celia, M. A., et al. Applicability of vertical-equilibrium and sharp-interface assumptions in CO_2 sequestration modeling. International Journal of Greenhouse Gas Control, 2012, 10: 134-147.

de Jonge-Anderson, I., Widyanita, A., Busch, A., et al. New Insights into the structural and stratigraphic evolution of the Malay Basin using 3D seismic data: Implications for regional carbon capture and storage potential. EarthArXiv Preprint, 2024.

De Silva, G. P. D., Ranjith, P. G., Perera, M. S. A. Geochemical aspects of CO_2 sequestration in deep saline aquifers: A review. Fuel, 2015, 155: 128-143.

Fenghour, A., Wakeham, W. A., Vesovic, V. The viscosity of carbon dioxide. Journal of Physical and Chemical Reference Data, 1998, 27(1): 31-44.

Gasda, S. E., Nordbotten, J. M., Celia, M. A. Vertical equilibrium with sub-scale analytical methods for geological CO_2 sequestration. Computational Geosciences, 2009, 13(4): 469-481.

Gasda, S. E., Nordbotten, J. M., Celia, M. A. Vertically averaged approaches for CO_2 migration with solubility trapping. Water Resources Research, 2011, 47(5): e2010WR009075.

Goodman, A., Hakala, A., Bromhal, G., et al. US DOE methodology for the development of geologic storage potential for carbon dioxide at the national and regional scale. International Journal of Greenhouse Gas Control, 2011, 5(4): 952-965.

Gorecki, C. D., Sorensen, J. A., Bremer, J. M., et al. Development of storage coefficients for determining the effective CO_2 storage resource in deep saline formations. Paper SPE 126444 Presented at SPE International Conference on CO_2 Capture, Storage, and Utilization, San Diego, California, USA, 2-4 November, 2009.

Hasbollah, D. Z. A., Junin, R., Taib, A. M., et al. Basin Evaluation of CO_2 Geological Storage Potential in Malay Basin, Malaysia, in Geotechnics for Sustainable Infrastructure Development, edited by P. Duc Long and N. T. Dung, Springer, Singapore, pp. 1405-1410, 2020.

Intergovernmental Panel on Climate Change (IPCC). Contribution of working groups I, II and III to the sixth assessment report of the intergovernmental panel on climate change. 2023.

Jackson, W. A., Hampson, G. J., Jacquemyn, C., et al. A screening assessment of the impact of sedimentological heterogeneity on CO_2 migration and stratigraphic-baffling potential: Johansen and Cook formations, Northern Lights project, offshore Norway. International Journal of Greenhouse Gas Control, 2022, 120: 103762.

Jin, Z. L., Durlofsky, L. J. Reduced-order modeling of CO_2 storage operations. International Journal of Greenhouse Gas Control, 2018, 68: 49-67.

Juanes, R., MacMinn, C. W., Szulczewski, M. L. The Footprint of the CO_2 Plume during Carbon Dioxide Storage in Saline Aquifers: Storage Efficiency for Capillary Trapping at the Basin Scale. Transport in Porous Media, 2010, 82(1): 19-30.

Kuttan, K., Stockbridge, C. P., Crocker, H., et al. Log interpretation in the Malay Basin. Paper SPWLA-1980-II Presented at SPWLA 21st Annual Logging Symposium, Lafayette, Louisiana, 8-11 July, 1980.

Lie, K. A. An Introduction to Reservoir Simulation Using MATLAB/GNU Octave: User Guide for the MATLAB Reservoir Simulation Toolbox (MRST). Cambridge, UK, University Press, 2019.

Lie, K. A., Nilsen, H. M., Andersen, O., et al. A simulation workflow for large-scale CO_2 storage in the Norwegian North Sea. Computational Geosciences, 2016, 20(3): 607-622.

Madon, M., Jong, J. Geothermal gradient and heat flow maps of offshore malaysia: Some updates and observations. Bulletin of the Geological Society of Malaysia, 2021, 71: 159-183.

Mathias, S. A., Gluyas, J. G., Goldthorpe, W. H., et al. Impact of Maximum Allowable Cost on CO_2 Storage Capacity in Saline Formations. Environmental Science & Technology, 2015, 49(22): 13510-13518.

Møyner, O., Nilsen, H. M. Multiresolution coupled vertical equilibrium model for fast flexible simulation of CO_2 storage. Computational Geosciences, 2019, 23(1): 1-20.

Nilsen, H. M., Herrera, P. A., Ashraf, M., et al. Field-case simulation of CO_2-plume migration using vertical-equilibrium models. Energy Procedia, 2011, 4: 3801-3808.

Nilsen, H. M., Krogstad, S., Andersen, O., et al. Using sensitivities and vertical-equilibrium models for parameter estimation of CO_2 injection models with application to sleipner data. Energy Procedia, 2017, 114: 3476-3495.

Nilsen, H. M., Lie, K. A., Andersen, O. Fully-implicit simulation of vertical-equilibrium models with hysteresis and capillary fringe. Computational Geosciences, 2016, 20: 49-67.

Nilsen, H. M., Lie, K. A., Møyner, O., et al. Spill-point analysis and structural trapping capacity in saline aquifers using MRST-co2lab. Computers & Geosciences, 2015, 75: 33-43.

Nordbotten, J. M., Celia, M. A. An improved analytical solution for interface upconing around a well. Water Resources Research, 2006, 42(8): e2005WR004738.

Nordbotten, J. M., Celia, M. A. Geological Storage of CO_2: Modeling Approaches for Large-scale Simulation. New Jersey, USA, John Wiley & Sons, 2011.

Nordbotten, J. M., Celia, M. A., Bachu, S. Injection and storage of CO_2 in deep saline aquifers: Analytical solution for CO_2 plume evolution during injection. Transport in Porous Media, 2005, 58(3): 339-360.

Nordbotten, J. M., Kavetski, D., Celia, M. A., et al. Model for CO_2 leakage including multiple geological layers and multiple leaky wells. Environmental Science & Technology, 2009, 43(3): 743-749.

Okwen, R., Stewart, M. T., Cunningham, J. A. Analytical solution for estimating storage efficiency of geologic sequestration of CO_2. International Journal of Greenhouse Gas Control, 2010, 4(1): 102-107.

Okwen, R., Yang, F., Frailey, S. Effect of geologic depositional environment on CO_2 storage efficiency. Energy Procedia, 2014, 63: 5247-5257.

Petrovskyy, D., Jacquemyn, C., Geiger, S., et al. Rapid flow diagnostics for prototyping of reservoir concepts and models for subsurface CO_2 storage. International Journal of Greenhouse Gas Control, 2023, 124: 103855.

Pooladi-Darvish, M., Moghdam, S., Xu, D. Multiwell injectivity for storage of CO_2 in aquifers. Energy Procedia, 2011, 4: 4252-4259.

Postma, T. J. W., Bandilla, K. W., Peters, C. A., et al. Field-scale modeling of CO_2 mineral trapping in reactive rocks: A vertically integrated approach. Water Resources Research, 2022, 58(1): e2021WR030626.

Span, R., Wagner, W. Equations of state for technical applications. I. Simultaneously optimized functional forms for nonpolar and polar fluids. International Journal of Thermophysics, 2003, 24(1): 1-39.

Szulczewski, M. L., MacMinn, C. W., Herzog, H. J., et al. Lifetime of carbon capture and storage as a climate-change mitigation technology. Proceedings of the National Academy of Sciences, 2012, 109(14): 5185-5189.

Szulczewski, M. L., MacMinn, C. W., Juanes, R. Theoretical analysis of how pressure buildup and CO_2 migration can both constrain storage capacity in deep saline aquifers. International Journal of Greenhouse Gas Control, 2014, 23: 113-118.

Thibeau, S., Mucha, V. Have we overestimated saline aquifer CO_2 storage capacities? Oil & Gas Science and Technology-Revue d'IFP Energies Nouvelles, 2011, 66(1): 81-92.

Vangkilde-Pedersen, T., Anthonsen, K. L., Smith, N., et al. Assessing European capacity for geological storage of carbon dioxide-the EU GeoCapacity project. Energy Procedia, 2009, 1(1): 2663-2670.

Zhou, Q., Birkholzer, J. T., Tsang, C. F., et al. A method for quick assessment of CO_2 storage capacity in closed and semi-closed saline formations. International Journal of Greenhouse Gas Control, 2008, 2(4): 626-639.